

## Nanoparticle Modification by Weak Polyelectrolytes for pH-Sensitive Pickering Emulsions

Martin F. Haase,<sup>\*,†</sup> Dmitry Grigoriev,<sup>†</sup> Helmuth Moehwald,<sup>†</sup> Brigitte Tiersch,<sup>‡</sup> and Dmitry G. Shchukin<sup>†</sup><sup>†</sup>Max Planck Institute of Colloids and Interfaces Am Mühlenberg 1, 14476 Potsdam-Golm, Germany, and<sup>‡</sup>Universität Potsdam - Institut für Chemie Karl-Liebknecht-Strasse 24-25, Haus 25, 14476 Potsdam-Golm, Germany

Received July 11, 2010. Revised Manuscript Received October 26, 2010

The affinity of weak polyelectrolyte coated oxide particles to the oil–water interface can be controlled by the degree of dissociation and the thickness of the weak polyelectrolyte layer. Thereby the oil in water (o/w) emulsification ability of the particles can be enabled. We selected the weak polyacid poly(methacrylic acid sodium salt) and the weak polybase poly(allylamine hydrochloride) for the surface modification of oppositely charged alumina and silica colloids, respectively. The isoelectric point and the pH range of colloidal stability of both particle–polyelectrolyte composites depend on the thickness of the weak polyelectrolyte layer. The pH-dependent wettability of a weak polyelectrolyte-coated oxide surface is characterized by contact angle measurements. The o/w emulsification properties of both particles for the nonpolar oil dodecane and the more polar oil diethylphthalate are investigated by measurements of the droplet size distributions. Highly stable emulsions can be obtained when the degree of dissociation of the weak polyelectrolyte is below 80%. Here the average droplet size depends on the degree of dissociation, and a minimum can be found when 15 to 45% of the monomer units are dissociated. The thickness of the adsorbed polyelectrolyte layer strongly influences the droplet size of dodecane/water emulsion droplets but has a less pronounced impact on the diethylphthalate/water droplets. We explain the dependency of the droplet size on the emulsion pH value and the polyelectrolyte coating thickness with arguments based on the particle-wetting properties, the particle aggregation state, and the oil phase polarity. Cryo-SEM visualization shows that the regularity of the densely packed particles on the oil–water interface correlates with the degree of dissociation of the corresponding polyelectrolyte.

## Introduction

For a century, it has been known that emulsions made of two immiscible liquids can be stabilized against coalescence<sup>1</sup> with solid particles. A stable emulsion consisting of these three components is generally denoted as a Pickering emulsion. However, particles can only act as emulsifiers when their surface chemistry and morphology offer wettability for both immiscible liquids. If this is the case and the particles initially dispersed in liquid (a) come into contact with the liquid–liquid interface, then they immerse partially into liquid (b). The extent of immersion is determined by the solid wettability properties of both liquids and can be expressed by the three-phase contact angle  $\theta_{ow}$ .<sup>2</sup>  $\theta_{ow}$  determines the energy of attachment of the particles to the interface, and the calculated energy reaches a maximum for spherical particles at  $\theta_{ow} = 90^\circ$ . The liquid with the poorer wettability becomes the dispersed phase. For a given liquid–liquid interfacial area, sufficient particles can order in a densely packed hexagonal arrangement. By reducing the interfacial area between two liquids, the interfacial energy of the system is also reduced.

For a given solid material and using water as the polar liquid, one can manipulate the polarity of the oil phase to vary  $\theta_{ow}$ . Binks and Clint<sup>3</sup> have shown changes of  $\theta_{ow}$  for dichlorodimethylsilane-

coated silica nanoparticles of intermediate hydrophobicity ranging from  $75^\circ$  for alkanes to  $150^\circ$  for oils containing ester and hydroxyl groups.

Often initially hydrophilic particles (e.g., silica, clays, and carboxylated or sulfonated latexes) are used for emulsification of oils in water. Here an accessible parameter to modify  $\theta_{ow}$  is the surface energy of the particles. Several research papers have described methods to do so, for example, by physi-<sup>4–6</sup> and chemisorption<sup>7–9</sup> of organic molecules or salt-induced compression of the particle electrical double layer.<sup>10–12</sup> A regulation of the pH value is in many cases necessary to control the charges of weak

(4) Binks, B. P.; Rodrigues, J. A.; Frith, W. J. Synergistic interaction in emulsions stabilized by a mixture of silica nanoparticles and cationic surfactant. *Langmuir* **2007**, *23*, 3626–3636.

(5) Cui, Z. G.; Shi, K. Z.; Cui, Y. Z.; Binks, B. P. Double phase inversion of emulsions stabilized by a mixture of CaCO<sub>3</sub> nanoparticles and sodium dodecyl sulphate. *Colloids Surf., A* **2008**, *329*, 67–74.

(6) Wang, J.; Yang, F.; Li, C. F.; Liu, S. Y.; Sun, D. J. Double phase inversion of emulsions containing layered double hydroxide particles induced by adsorption of sodium dodecyl sulfate. *Langmuir* **2008**, *24*, 10054–10061.

(7) Binks, B. P.; Lumsdon, S. O. Influence of particle wettability on the type and stability of surfactant-free emulsions. *Langmuir* **2000**, *16*, 8622–8631.

(8) Binks, B. P.; Whitby, C. P. Silica particle-stabilized emulsions of silicone oil and water: aspects of emulsification. *Langmuir* **2004**, *20*, 1130–1137.

(9) Saleh, N.; Sarbu, T.; Sirk, K.; Lowry, G. V.; Matyjaszewski, K.; Tilton, R. D. Oil-in-water emulsions stabilized by highly charged polyelectrolyte-grafted silica nanoparticles. *Langmuir* **2005**, *21*, 9873–9878.

(10) Ashby, N. P.; Binks, B. P. Pickering emulsions stabilised by Laponite clay particles. *Phys. Chem. Chem. Phys.* **2000**, *2*, 5640–5646.

(11) Frith, W. J.; Pichot, R.; Kirkland, M.; Wolf, B. Formation, stability, and rheology of particle stabilized emulsions: influence of multivalent cations. *Ind. Eng. Chem. Res.* **2008**, *47*, 6434–6444.

(12) Yang, F.; Liu, S. Y.; Xu, J.; Lan, Q.; Wei, F.; Sun, D. J. Pickering emulsions stabilized solely by layered double hydroxides particles: the effect of salt on emulsion formation and stability. *J. Colloid Interface Sci.* **2006**, *302*, 159–169.

\*To whom correspondence should be addressed. E-mail: martin.haase@mpikg.mpg.de.

(1) Pickering, S. U. Emulsions. *J. Chem. Soc.* **1907**, *91*, 2001–2021.

(2) Schulman, J. H.; Leja, J. Control of contact angles at the oil-water-solid interfaces - emulsions stabilized by solid particles (BaSO<sub>4</sub>). *Trans. Faraday Soc.* **1954**, *50*, 598–605.

(3) Binks, B. P.; Clint, J. H. Solid wettability from surface energy components: relevance to pickering emulsions. *Langmuir* **2002**, *18*, 1270–1273.

acid or base groups in the system and thereby the particle emulsification ability. This can be the case for physisorbed amphiphiles,<sup>13–15</sup> the bare particle surface,<sup>16,17</sup> grafted weak polyelectrolytes (PEs)<sup>18–22</sup> or microgel particles consisting of weak PEs.<sup>23–26</sup> Therefore, two basic concepts to increase the surface lipophilicity can be pointed out: (i) the introduction of hydrophobic moieties onto the surface and (ii) the compensation of the effective charge density on the surface.

With the present work, we extend the diversified methods of particle surface wettability modification with a simple method involving weak PE modification of the initially hydrophilic colloidal particle surface. This attempt is in particular comparable to the works of Armes et al.<sup>18–21</sup> dealing with grafting of weak PEs onto the particle surface to enable their emulsification ability. However, the main differences of the present work are (i) the method of weak PE deposition (done by a simple one step physisorption), (ii) their conformation and amount on the surface (due to changes of the conditions during the physisorption step), and (iii) the different polymers used here. Compared with attempts of particle hydrophobization with, for example, amphiphiles, the modification of the particle surface with weak PEs brings the advantage of amphiphile-free liquid phases.

Weak PE adsorption onto planar and particle surfaces has been an important field of research during the last two decades. Their

ability to improve dispersibility of different powders in water has been shown in several publications,<sup>27–30</sup> and since Decher and Hong<sup>31</sup> introduced the layer-by-layer technique, the number of publications per year has increased exponentially.

Weak PEs typically consist of a nonpolar hydrocarbon backbone and polar functional groups with a pH-dependent degree of dissociation. By controlling the charge of the PE, the hydrophilic contribution of the dissociable functional groups and thereby the PE affinity to oil–water interfaces can be governed. Therefore, weak PEs physisorbed onto hydrophilic solid particles provide a proper surface modification to control the wetting properties<sup>32</sup> of these particles and thereby their emulsification ability.

By depositing one layer of weak PEs, we can control the affinity of colloidal particles to the oil/water interface by adjusting the pH value and thereby the degree of dissociation in the PE layer (Scheme 1A).

Furthermore, we study the different emulsification properties of colloidal particles carrying a PE layer of different thickness (Scheme 1B). To show the generality, we demonstrate the emulsification ability for both possible combinations: (i) weak polyacid and positively charged particles and (ii) weak polybase and negatively charged particles. Because wettability depends on the degree of dissociation of the PE, stable emulsions can only be obtained in a certain pH window, which depends on the type of the PE.

After 20 years of research on time-consuming PE-multilayer deposition, this attempt reveals again one successful application of an easily fabricable surface modification by a thin weak PE single layer.

## Experimental Section

**Materials.** Ludox TMA suspension (average particle diameter: from BET sorption data (134 m<sup>2</sup>/g, 2.34 g/mL) 19.1 nm, obtained by DLS measurements 16 nm), alumina nanoparticle suspension (particle diameter: from BET sorption data (396 m<sup>2</sup>/g, 3.94 g/mL) 4 nm, obtained by DLS measurements 16 nm), poly(allylamine hydrochloride) (PAH, average MW ≈ 17 000 g/mol), poly(methacrylic acid, sodium salt) solution (PMAA, average MW by GPC ≈ 9500 g/mol), and diethylphthalate (99.5%) were purchased from Sigma-Aldrich and used as received. Dodecane (99+%, Sigma Aldrich) was purified from polar impurities by mixing twice with activated basic alumina (5016 Brockmann 1 stand grade), and removal of solid was done with a folded filter. Diluted sodium hydroxide and hydrochloric acid (Titripur from Merck) were used to adjust the pH. Water was purified before use in a three-stage Millipore Milli-Q Plus 185 purification system and had a conductivity < 18.2 MΩ·cm<sup>-1</sup>.

**PE Adsorption at Constant pH and Removal of Excess PE.** A stock solution of 5 wt % PMAA-NaCl and 4 wt % PAH, respectively, was diluted in water with an appropriate volume of 1 M HCl or NaOH, respectively, to obtain the desired pH value (PMAA-NaCl: pH 4, 5, 6, 7; PAH: pH 8, 8.5, 9.5). The same pH adjustment was done for 8 wt % alumina and 20 wt % Ludox TMA dispersion. The particle suspensions were added dropwise to the PE stock solutions with the same pH value under vigorous stirring. During this addition, the pH value was monitored continuously with a calibrated pH electrode (WTW SenTix Mic) and maintained by the addition of either 1 M HCl (alumina–PMAA) or 1 M NaOH (silica–PAH) with a maximum deviation

(13) Akartuna, I.; Studart, A. R.; Tervoort, E.; Gonzenbach, U. T.; Gauckler, L. J. Stabilization of oil-in-water emulsions by colloidal particles modified with short amphiphiles. *Langmuir* **2008**, *24*, 7161–7168.

(14) Lan, Q.; Liu, C.; Yang, F.; Liu, S. Y.; Xu, J.; Sun, D. J. Synthesis of bilayer oleic acid-coated Fe<sub>3</sub>O<sub>4</sub> nanoparticles and their application in pH-responsive Pickering emulsions. *J. Colloid Interface Sci.* **2007**, *310*, 260–269.

(15) Li, J.; Stover, H. D. H. Doubly pH-Responsive Pickering Emulsion. *Langmuir* **2008**, *24*(23), 13237–13240.

(16) Binks, B. P.; Rodrigues, J. A. Inversion of emulsions stabilized solely by ionizable nanoparticles. *Angew. Chem., Int. Ed.* **2005**, *44*, 441–444.

(17) Wolf, B.; Lam, S.; Kirkland, M.; Frith, W. J. Shear thickening of an emulsion stabilized with hydrophilic silica particles. *J. Rheol.* **2007**, *51*, 465–478.

(18) Dupin, D.; Armes, S. P.; Connan, C.; Reeve, P.; Baxter, S. M. How does the nature of the steric stabilizer affect the pickering emulsifier performance of lightly cross-linked, acid-swallowable poly(2-vinylpyridine) latexes? *Langmuir* **2007**, *23*, 6903–6910.

(19) Fujii, S.; Randall, D. P.; Armes, S. P. Synthesis of polystyrene/poly[2-(dimethylamino) ethyl methacrylate-*stat*-ethylene glycol dimethacrylate] core-shell latex particles by seeded emulsion polymerization and their application as stimulus-responsive particulate emulsifiers for oil-in-water emulsions. *Langmuir* **2004**, *20*, 11329–11335.

(20) Read, E. S.; Fujii, S.; Amalvy, J. I.; Randall, D. P.; Armes, S. P. Effect of varying the oil phase on the behavior of pH-responsive latex-based emulsifiers: demulsification versus transitional phase inversion. *Langmuir* **2004**, *20*, 7422–7429.

(21) Read, E. S.; Fujii, S.; Amalvy, J. I.; Randall, D. P.; Armes, S. P. Effect of varying the oil phase on the behavior of pH-responsive latex-based emulsifiers: demulsification versus transitional phase inversion. *Langmuir* **2005**, *21*, 1662–1662.

(22) Zhang, J.; Chen, K. Q.; Zhao, H. Y. PMMA colloid particles armored by clay layers with PDMAEMA polymer brushes. *J. Polym. Sci., Polym. Chem.* **2008**, *46*, 2632–2639.

(23) Binks, B. P.; Murakami, R.; Armes, S. P.; Fujii, S. Effects of pH and salt concentration on oil-in-water emulsions stabilized solely by nanocomposite microgel particles. *Langmuir* **2006**, *22*, 2050–2057.

(24) Brugger, B.; Richtering, W. Emulsions stabilized by stimuli-sensitive poly(*N*-isopropylacrylamide)-*co*-methacrylic acid polymers: microgels versus low molecular weight polymers. *Langmuir* **2008**, *24*, 7769–7777.

(25) Fujii, S.; Armes, S. P.; Binks, B. P.; Murakami, R. Stimulus-responsive particulate emulsifiers based on lightly cross-linked poly(4-vinylpyridine)-silica nanocomposite microgels. *Langmuir* **2006**, *22*, 6818–6825.

(26) Ngai, T.; Auweter, H.; Behrens, S. H. Environmental responsiveness of microgel particles and particle-stabilized emulsions. *Macromolecules* **2006**, *39*, 8171–8177.

(27) Cesarano, J.; Aksay, I. A.; Bleier, A. Stability of Aqueous α-Al<sub>2</sub>O<sub>3</sub> suspensions with poly(methacrylic acid) polyelectrolyte. *J. Am. Ceram. Soc.* **1988**, *71*, 250–255.

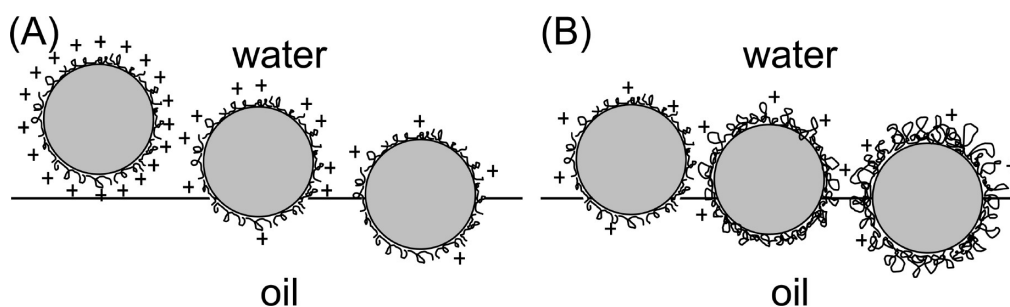
(28) Hackley, V. A. Colloidal processing of silicon nitride with poly(acrylic acid): I. Adsorption and electrostatic interactions. *J. Am. Ceram. Soc.* **1997**, *80*, 2315–2325.

(29) Lopez, M. C. B.; Rand, B.; Riley, F. L. Polymeric stabilisation of aqueous suspensions of barium titanate. Part I: Effect of pH. *J. European Ceram. Soc.* **2000**, *20*, 1579–1586.

(30) Zhang, J. X.; Duan, L. P.; Jiang, D. L.; Lin, Q. L.; Iwasa, M. Dispersion of TiN in aqueous media. *J. Colloid Interface Sci.* **2005**, *286*, 209–215.

(31) Decher, G.; Hong, J. D.; Schmitt, J. Buildup of ultrathin multilayer films by a self-assembly process: III. Consecutively alternating adsorption of anionic and cationic polyelectrolytes on charged surfaces. *Thin Solid Films* **1992**, *210*, 831–835.

(32) Burke, S. E.; Barrett, C. J. pH-Responsive properties of multilayered poly(L-lysine)/hyaluronic acid surfaces. *Biomacromolecules* **2003**, *4*, 1773–1783.

Scheme 1<sup>a</sup>

<sup>a</sup>The affinity of a nanoparticle carrying an adsorbed layer of a weak PE can be modified by (A) the degree of dissociation of the weak PE and (B) the thickness of the adsorbed PE layer.

of  $\pm 0.1$  pH units from the desired pH value. This pH value, where the coating occurs, is abbreviated as  $\text{pH}_C$ , where C in the index stands for PE-coating. This  $\text{pH}_C$  value is to be distinguished from the pH value during emulsification. The addition of the particle suspension was finished when the particle mass-fraction reached 5 wt % (alumina–PMAA) or 10 wt % (silica–PAH), respectively. All suspensions were gelated during this treatment and were sonicated in an ultrasonic bath for 20 min afterward. The suspensions were subsequently ultracentrifuged for 1 h at 30 000 rpm (RCF 82700) in an ultracentrifuge (Beckmann L70 ultracentrifuge). The clear supernatant was removed, and the sediment was redispersed in ultrapure water via sonication (Ultrasonic Processor VCX 505, Sonics & Materials, Inc., USA, 20kHz, 500W, 10 mm tip-diameter). Two more centrifugations at 30 000 rpm followed each one for 3 h. The suspension of redispersed nanoparticles became less turbid with each washing cycle, and optically clear suspensions were obtained (representing a low degree of nanoparticle aggregation) after the third redispersion. The excessive washing procedure here was mainly applied to show later in this work that emulsification occurs only because of PE-modified particles and not because of free polymer in solution. For practical purposes, one washing step can also be sufficient.

**Measurement of Electrophoretic Mobility.** A small volume of the washed particle suspensions was diluted to obtain a 0.2 wt % suspension. A magnetic stir bar was added to the suspension, and the pH was adjusted by the addition of HCl or NaOH, respectively. Samples of 1 mL were taken and transferred to a 2 mL centrifuge tube. The pH value was measured before the sample was transferred to a DTS 1060C cell. The electrophoretic mobility was measured in this cell with a Malvern ZetaSizer Nano ZS, equipped with a laser operating at 533 nm.

**Contact Angle Measurements.** Polished alumina plates were purchased from MTI Corporation (size  $10 \times 10 \times 1 \text{ mm}^3$ , crystal orientation 0001). The plates were rinsed with acetone, ethanol, and ultrapure water. The PMAA deposition was done by dip coating the plates for 10 min in a 2 wt % aqueous PMAA solution with pH 6 or 4. Three consecutive washing steps, each one for 5 min in ultrapure water, followed. For the contact angle measurements, the plates were immersed in a 1 mM NaCl solution with a defined pH and after that dried in a nitrogen flow. The plates were then transferred in a quartz cell filled with dodecane. Contact angles were measured on a Krüss contact angle measuring system G10. A drop of the NaCl solution was placed via a microsyringe on the center of the plate. The droplet volume was increased via a pump, and photographs of the droplet with a CCD video camera (Zoom 1:6.5) were taken. The advancing contact angle was then evaluated with the plugin LB-ADSA (École Polytechnique Fédérale de Lausanne) for the graphical software imageJ.

**Preparation of Emulsions.** Appropriate volumes of the washed PE-modified particle suspensions were diluted in 2 mL Eppendorf centrifuge tubes to obtain 1.5 mL of 2 wt % alumina or silica suspensions at the desired pH value. Then, 0.5 mL of the oil

phase was added (dodecane or diethylphthalate), and a pre-emulsification was done by shaking in a vortex for 10 min. After that, the emulsions were sonicated with an ultrasonic processor (Ultrasonic processor Sonopuls HD200, Bandel-Germany, 20kHz, 200W, 2 mm tip-diameter) for 4 min. The emulsions were cooled in a stirred ice bath during the emulsification. Samples were characterized 12 h after preparation. Each emulsification was performed at the same ultrasonic intensity, emulsification time, emulsion volume, dipping depth of the sonotrode, and cooling rate. Only the type of PE-modified particles (alumina, silica, PE,  $\text{pH}_C$ ) and aqueous pH value was varied.

**Measurement of Droplet Size Distribution.** A drop of the emulsion was investigated with an optical microscope (Olympus BH-2) with a dark field device at a magnification of  $40\times$ . Ten micrographs per sample were taken by means of a camera (Olympus C-5050Zoom) with additional optical zoom of  $5\times$ . The software imageJ was used for the analysis of the micrographs, containing steps such as contrasting, subtracting background, binarization, and numerical evaluation of droplet cross sectional area. The droplet diameter was calculated, and a droplet size distribution was obtained. At least 3000 drops per sample were counted.

**Cryo-SEM Visualization of Droplet Morphology.** The morphology of the emulsion droplets was examined by cryo-high-resolution scanning electron microscopy (cryo-SEM). Each sample was cooled by plunging into nitrogen slush at atmospheric pressure. The samples were freeze-fractured at  $-150^\circ\text{C}$ , etched for 60 s at  $-98^\circ\text{C}$ , sputtered with platinum in the GATAN Alto 2500 Cryo preparation chamber, and then transferred into the Cryo-SEM.

## Results and Discussion

**Characterization of PE-Modified Particles.** Cesarano et al.<sup>27</sup> studied the adsorption of PMAA (15 000 g/mol) onto alumina and found the adsorbed amount to depend strongly on the pH value during the adsorption step. With a decreasing pH value the adsorbed PMAA amount increases greatly, in particular in the pH region in which the degree of dissociation ( $\alpha$ ) of the PMAA acid groups changes dramatically (pH 3–6). Decreasing  $\alpha$  leads to an increased coiling of PMAA in solution and thereby to an increased amount of adsorbed PE's per surface area (thicker PE layer). This concept can be generalized to the adsorption behavior of PAH on silica. The only differences are the different pH range and the reverse pH direction for a decreasing charge.

To guarantee the adsorbed amount of PMAA to be as high as possible for each pH value during the PE coating step ( $\text{pH}_C$ ), we selected the PMAA concentration to provide excess PMAA. (See the Supporting Information (SI).) Washing of the PE-modified particles ensures removal of excess PE due to dilution. Dynamic light scattering measurements of the PMAA-coated alumina particles (obtained after washing, see SI) show that the extent of

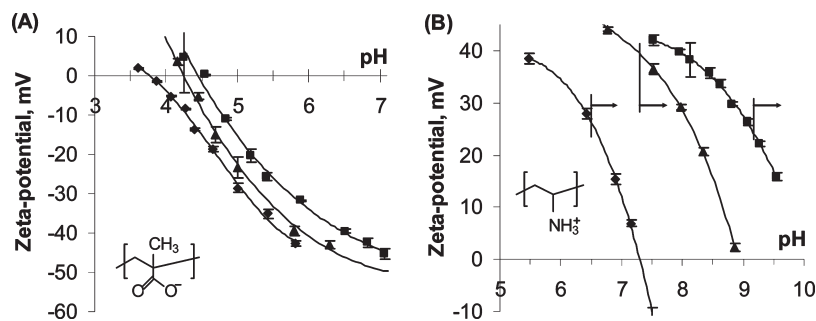


**Figure 1.** pH dependence of the zeta potential for PE-coated nanoparticles with different pH values of PE coating ( $\text{pH}_C$ ): (A) PMAA-coated alumina: ■,  $\text{pH}_C$  7.0; ▲,  $\text{pH}_C$  6.0; ◆,  $\text{pH}_C$  4.0 ( $\text{pH}_C$  5 excluded to prevent overcrowding, see the SI); (B) PAH-coated silica: ■,  $\text{pH}_C$  9.5; ▲,  $\text{pH}_C$  8.0; ◆,  $\text{pH}_C$  7. Vertical lines with arrows show the pH value where the occurrence of turbidity was observed. For alumina–PMAA, this takes place for  $\text{pH}_C$  7, 6, 5, 4 at pH 5.6, 5.3, 4.5, and 4.0, respectively. Error bars give standard deviation of five measurements.

particle aggregation is low and is of the same order as that for the bare alumina particles.

After washing, the measured zeta potential of the PE-modified particles should be influenced only by the contribution of the pH-dependent dissociation of the adsorbed PE, the underlying oxide particle surface, and the ionic strength. The results of zeta potential measurements are shown in Figure 1A,B for PMAA-coated alumina and PAH-coated silica particles, respectively.

Alumina particles themselves have an isoelectric point (IEP) at  $\text{pH} \sim 9$  and are positively charged in the range of the pH values displayed in Figure 1A, whereas the IEP of silica particles can be found at  $\text{pH} \sim 2$ , and their surface is negatively charged at the pH values displayed in Figure 1B. With the PEs on the surface, the zeta potential sign of the particles is reversed. By changing the pH value to decrease  $\alpha$  of the adsorbed PE, the zeta potential in absolute value decreases. The sign is reversed to the charge corresponding to the bare particle surface at the IEP of the PE/particle composite.

From Figure 1, three main conclusions, valid for both PE–particle combinations, can be drawn: With decreasing  $\alpha$  of the PE (increasing  $\text{pH}_C$  for PAH, decreasing  $\text{pH}_C$  for PMAA) during the adsorption step, (i) the IEP shifts toward pH values corresponding to lower  $\alpha$ , (ii) the absolute value of the zeta potential of the particles with a charged PE layer is higher for the same pH value, and (iii) particle flocculation in the suspension occurs at pH values with a lower corresponding  $\alpha$ .

These conclusions can be explained by the  $\text{pH}_C$ -dependent amount of adsorbed PE on the surface, as described at the beginning of this section. With lower  $\alpha$  during the PE adsorption step, a larger amount of the PE per surface area is adsorbed (thicker PE layer). It can be concluded therefore that thicker PE layers provide more charges per surface area at a given pH value. This explains the higher absolute zeta potentials for thicker layers at similar pH values. For thick layers, even at low values of  $\alpha$ , there is still sufficient total charge to compensate for the counteracting charge of the bare particle surface. Because of that, the IEP of the particles is shifted.

We denote the pH value for the occurrence of turbidity in the suspension as the critical flocculation pH (c.f.pH) and observe a broader pH-dependent stability window for thicker layers. For many electrostatically stabilized particles, an absolute zeta potential above 30–35 mV provides good stability. For  $\text{pH}_C$  values of the systems, alumina–PMAA above  $\text{pH}_C$  6 and silica–PAH below  $\text{pH}_C$  8, this is the case, but for PE layers deposited at very low values of  $\alpha$ , colloidal stability is also achieved at absolute values of the zeta potential below 30 mV for alumina–PMAA of  $\text{pH}_C$  4 and even at an absolute zeta potential below 10 mV. A possible explanation could still be the electrostatic repulsion of

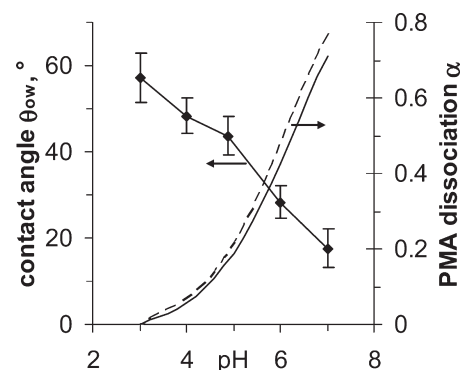


**Figure 2.** Advancing contact angles (left axis) of water droplets of different pH values under dodecane on a PMAA-coated ( $\text{pH}_C$  4) alumina plate. Error bars correspond to the standard deviation calculated from at least five measurements. Degree of dissociation of dissolved (nonadsorbed) PMAA (right axis) in (i) 1 (continuous line) and (ii) 10 mM (dashed line) NaCl taken from ref 28.

two overlapping thick PE layers of two particles. Even if  $\alpha$  is too low to enable the loops and tails of the adsorbed PE, a strong contribution to the electrophoretic mobility, charges inside the thick PE layer can provide repulsive interaction of two overlapping layers. This repulsive effect may also be enhanced by steric stabilization due to a contribution of an osmotic pressure for water. The penetration of water molecules into the PE layer moves the overlapping PE layers apart.

For uncharged PEs at pH values away from the IEP of the PE modified particles, the charge of the oxide particle surface dominates the zeta potential. One might expect that the PEs desorb from the surface, but experimental evidence (see SI) and the ability of the particles to emulsify oils in this pH range (Characterization of Emulsions section) confirm the maintenance of the adsorbed state here. The particles alone, at such pH values, could not achieve this, supporting the assumption that PEs remain adsorbed. van der Waals interactions, hydrogen bonding, or both are likely responsible for the maintenance of this adsorbed state. Desorption might also be unfavorable because of the low solubility of the uncharged PE in water.

**Wetting Properties of PMAA-Coated Alumina.** Contact angle measurements of water droplets (1 mM NaCl, varying pH) under dodecane on a polished alumina plate were carried out to demonstrate the effect of the charge density of the PE layer on the wettability of the particle surface. Figure 2 shows the pH dependency of the contact angle on a PMAA-coated alumina plate ( $\text{pH}_C$  4).

A comparison of the pH dependency of the contact angle with the degree of dissociation of the free PMAA<sup>28</sup> can be used to help our interpretation (Figure 2). However, when doing this comparison, it

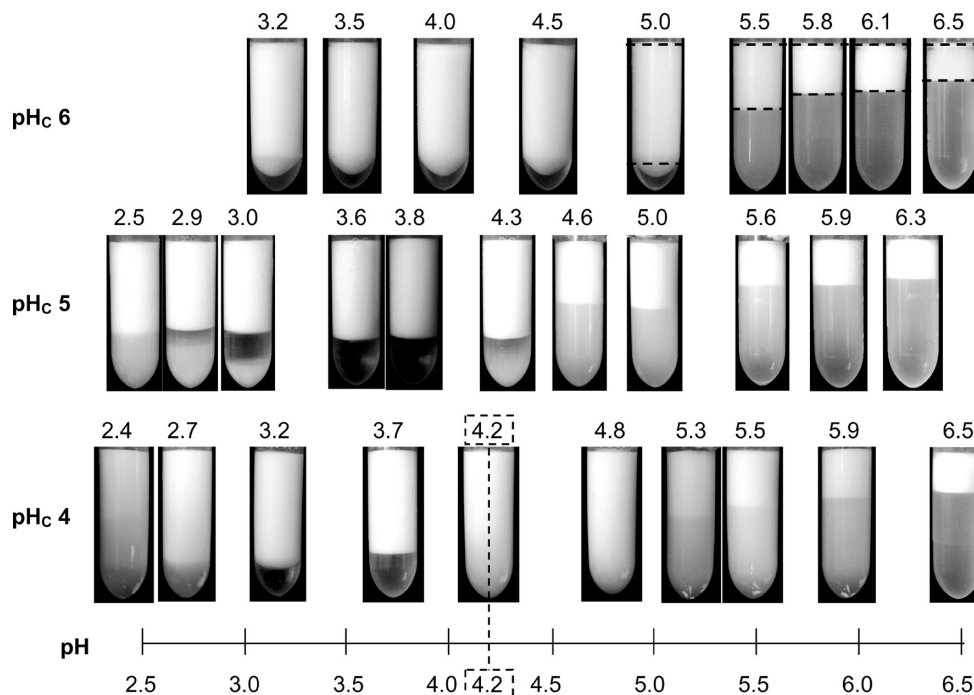


**Figure 3.** Photographs of 25 vol % dodecane/water emulsions stabilized with 2 wt % PMAA-coated alumina nanoparticles with different PE coating pH values ( $\text{pH}_C$  values) after 12 h of storage. (All emulsions prepared below pH 6.2 do not release oil after 3 months.) The vertical axis of the sample tube images corresponds to the pH axis at the bottom of the Figure, as indicated for the sample with pH 4.2 at  $\text{pH}_C$  4; precise pH values of samples are above the photographs. The arrangement of the sample photographs shows the increasing height of the creamed emulsion phase (indicated by dashed bars for photographs of  $\text{pH}_C$  6) with decreasing pH, the achievement of a maximum creaming layer height at lower pH when  $\text{pH}_C$  is lower, the formation of a sediment at pH 3, and its redispersion at even lower pH values.

is important to recognize that the pH dependency of the PMAA dissociation in the adsorbed state might differ slightly from that of the dissolved nonadsorbed PMAA. The increase in contact angle with decreasing pH comes along with a decrease in the charge density of the PMAA layer. For pH 5–7, the slope of contact angle dependency is higher than that for pH 3–5. A similar observation can be made for the slope of the  $\alpha$ -curve of free PMAA in this pH ranges. Therefore, we can conclude that the wettability of the surface for water or oil respectively correlates with the degree of dissociation of the PE layer.

Contact angle measurements were also performed for the uncoated alumina plate. (See the SI.) A contact angle of  $\sim 60^\circ$  was found, which was observed to be not pH-dependent within the range investigated. This surprisingly high contact angle can be explained by surface active contaminations in, for example, dodecane. Alumina is a typical example of a high energy surface that is sensitive to contamination. The same is the case for PMAA-coated alumina with  $\text{pH}_C$  6. Here the adsorbed amount of PMAA is not seen to provide sufficient compensation of the high-energy properties of the underlying alumina surface. This is contrary to the zeta potential measurements, in which the surface charge is observed to be governed by the adsorbed PMAA layer. We can conclude that there is a transition from a high to a low energy surface with increasing PE thickness.

**Characterization of Emulsions.** To prepare the emulsion samples, first the aqueous components were mixed, and depending on the pH, colloidal or gelled suspensions of nanoparticles in water were obtained. Figure 3 shows photographs of dodecane in water emulsions prepared with alumina–PMAA of different  $\text{pH}_C$  values (PE coating thickness increases with decreasing  $\text{pH}_C$ ) after emulsification by sonication at different emulsification pH values.

For the three different PE coating thicknesses ( $\text{pH}_C$  values), stable emulsions could be obtained below a pH value of  $\sim 6.7$  with

a corresponding  $\alpha^{27}$  of 0.7 (no salt) or 0.84 (10 mM NaCl). Samples emulsified above this pH value coalesce rapidly and create two separated liquid phases in  $< 5$  min, probably because of the predominantly hydrophilic character of the PMAA layer with  $\alpha > 0.8$ . By decreasing the pH value below 6,  $\alpha$  falls below 0.5, and the hydrophobic character of PMAA increases. Please note that the alumina particles themselves are not capable of stabilizing dodecane in water emulsions at any of the shown pH values.

The height of the creamed emulsion phase for particles of any  $\text{pH}_C$  value increases gradually with decreasing pH value after 12 h of storage until a maximum is reached. For samples with pH values above this maximum, further creaming after 12 h leads to a creaming layer occupying about 1/4 of the vials. The different creaming rates here can be explained with different droplet sizes and extents of droplet flocculation. (See Figures 4 and 5 and the SI.) It can also be seen that the turbidity of the aqueous phase below the creamed layer has increased in comparison with the initial suspension of the alumina–PMAA particles. Cryo SEM measurements (SI) confirm, in particular for  $\text{pH}_C$  5 and 4, that the particles are aggregated. The initial PMAA-coated particles are not aggregated, so we conclude that aggregation takes place during emulsification.

At a certain pH (depending on the PE coating thickness), a maximum creaming layer height is achieved. The aqueous phase for this state is not turbid (also no Rayleigh scattering) and therefore does not contain particles. The comparison of this pH value with the critical flocculation pH (c.f.pH) in Figure 1A shows correlation. Horozov and Binks<sup>33</sup> observed a similar effect but used hydrophobized silica nanoparticles at a certain ionic strength

(33) Horozov, T. S.; Binks, B. P.; Gottschalk-Gaudig, T. Effect of electrolyte in silicone oil-in-water emulsions stabilised by fumed silica particles. *Phys. Chem. Chem. Phys.* **2007**, *9*, 6398–6404.

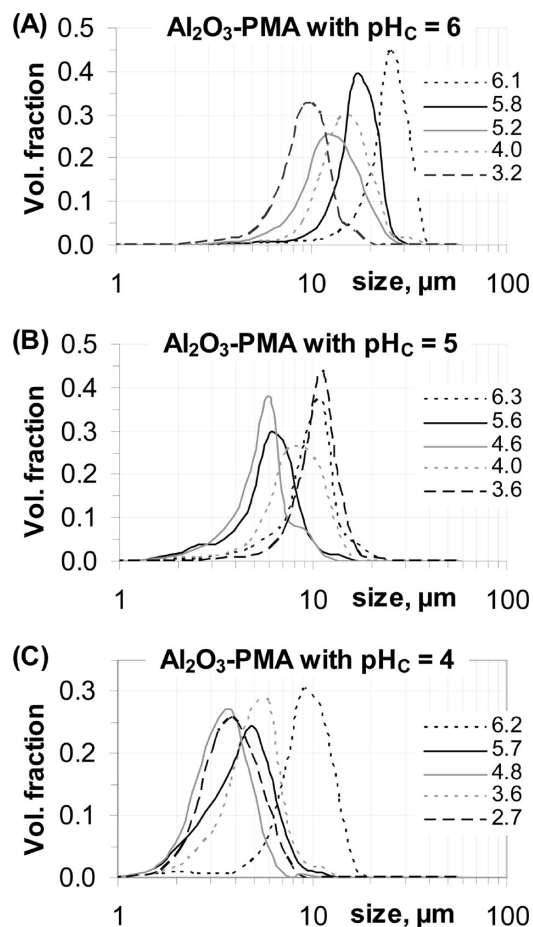


**Figure 4.** Size distributions of dodecane/water emulsion droplets stabilized by PMAA-coated alumina nanoparticles with different PMAA coating pH values  $pH_C$ : (A)  $pH_C$  6, (B)  $pH_C$  5, and (C)  $pH_C$  4 and for different emulsification pH values (designated by line pattern).

that corresponded to the critical flocculation concentration (cfc). Measurements of the resolved water fraction and the rheological properties of the emulsion led to the conclusion that above the cfc a viscoelastic 3D network of interconnected particles and emulsion droplets develops, which abruptly increases the stability against further creaming. Here we observe a similar phenomenon but by studying the PE-covered particles at their c.f.pH. As already shown in Figure 1A, with increasing PE coating thickness (decreasing  $pH_C$ ), the c.f.pH shifts to lower values. This is also the case for the pH value where the formation of the particle-droplet network occurs. Such analogous behavior can be found for the dodecane in water emulsion stabilized with silica-PAH particles, only in the more alkaline region above pH 6.5 corresponding to the c.f.pH marked in Figure 1B.

For the samples with intermediate PE coating thickness ( $pH_C$  5) at  $pH < 3$ , a whitish sediment of aggregated particles at the tube bottom can be observed. However, a further decrease in pH value leads again to the formation of a stable turbid aqueous phase. In the case of samples with the thickest PE coating ( $pH_C$  4), only a stable turbidity without sediment is observed. In both cases, the increasing positive zeta potential provides electrostatic restabilization of the excess particles. In all cases, the emulsions are still stable, indicating that the PEs are still adsorbed to the particle surface. The oil wetting ability of the bare alumina surface is poor in this pH range due to the strong surface charge but the uncharged PE layer provides sufficient hydrophobicity to stabilize the emulsions.

A separation of a distinguishable upper cream layer did not occur after 12 h of storage for emulsions stabilized with particles carrying the thickest PE coating ( $pH_C$  4) in the range of  $4.2 < pH < 5$ . This is due to the formation of unflocculated small droplets (SI), which have a slower rate of creaming.

The droplet size distribution for each sample was measured, and the obtained size distributions for alumina-PMAA are shown in Figure 4 for different  $pH_C$  and emulsification pH values.

All obtained droplet size distributions are monomodal when plotted as volume fraction. The droplet size distribution did not change after emulsification times  $> 4$  min.

During emulsification, the interplay between the stabilization of newly generated droplets and their coalescence determines the droplet size distribution. Depending on which process is dominant, the droplet size distribution shifts to smaller or bigger sizes.

Because emulsification is performed with high-intensity ultrasound, the break-up of droplets occurs because of the disruptive mechanical effects of acoustic cavitation. Droplet break-up goes along with increasing interfacial area. Because this is energetically unfavorable, the emulsion attempts to reduce the interfacial area again by coalescence of droplets. The higher the interfacial tension between water and oil, the faster the coalescence will proceed at a constant viscosity.

However, in the presence of interfacially active particles, coalescence can be suppressed because of the formation of an attached particle barrier on the newly generated oil-water interface. The magnitude of this droplet stabilization depends on the availability of particles and their rate of deposition on the interface. The availability is proportional to the particle concentration, and it has been found that the obtainable droplet size depends on this parameter.<sup>8,34–36</sup> Because of decreasing droplet sizes, the overall droplet surface area increases, and so does the required quantity of particles for coverage. However, for the case of a particle excess during emulsification, their concentration determines the amount of particles and their average distance to uncovered droplet interfaces. The rate of deposition of the particles on the interface is determined by (i) their affinity to the interface and (ii) their size. Both parameters affect the time required to cover uncovered oil-water interfaces.

Because emulsification was always performed under the same conditions (ultrasonic intensity, emulsification time, emulsion volume, dipping depth of the sonotrode, cooling rate, oil volume-content, and particle concentration), the droplet size distributions here are determined only by the properties of the particles and the oil phase. For PMAA-coated alumina particles of all PE coating thicknesses ( $pH_C$  values), the droplet size first decreases below pH 7. This observation is better illustrated in Figure 5A, where the average volumetrically weighted diameter of the droplets is plotted versus the pH value of the emulsions.

The decreasing pH causes a decreasing  $\alpha$  in the adsorbed PMAA coating.  $\alpha$  of PMAA can be linked to the three phase contact angle ( $\theta_{ow}$ ), as shown in Figure 2. Because for decreasing  $\alpha$  we observe a decreasing average droplet size, we propose the parameter  $\theta_{ow}$  to influence the droplet size distributions obtained here. As previously mentioned, in the pH range above the c.f.pH, particle aggregation during emulsification takes place. The resulting aggregates are submicrometer-sized. (See the SI.) This de-

(34) Arditty, S.; Whitby, C. P.; Binks, B. P.; Schmitt, V.; Leal-Calderon, F. Some general features of limited coalescence in solid-stabilized emulsions. *Eur. Phys. J. E* **2003**, *11*, 273–281.

(35) Melle, S.; Lask, M.; Fuller, G. G. Pickering emulsions with controllable stability. *Langmuir* **2005**, *21*, 2158–2162.

(36) Golemanov, K.; Tcholakova, S.; Kralchevsky, P. A.; Ananthapadmanabhan, K. P.; Lips, A. Latex-particle-stabilized emulsions of anti-Bancroft type. *Langmuir* **2006**, *22*, 4968–4977.

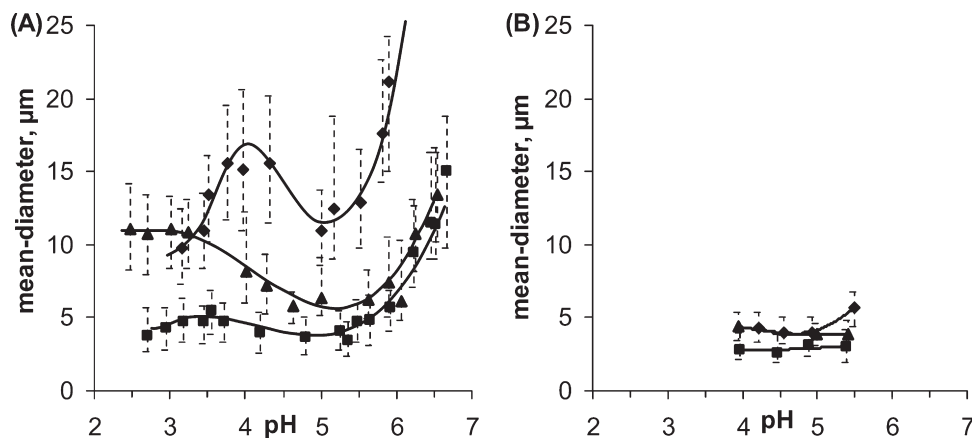


**Figure 5.** Mean volumetric diameter of emulsion droplets stabilized by PMAA-coated alumina nanoparticles with different coating pH values  $pH_C$ :  $\blacklozenge$ ,  $pH_C$  6.0;  $\blacktriangle$ ,  $pH_C$  5.0;  $\blacksquare$ ,  $pH_C$  4.0. (A) Dodecane as oil phase and (B) diethylphthalate as oil phase. Lines are drawn to guide the eye; dashed bars give upper and lower diameter at 50% height of the size distributions, not the error bars.

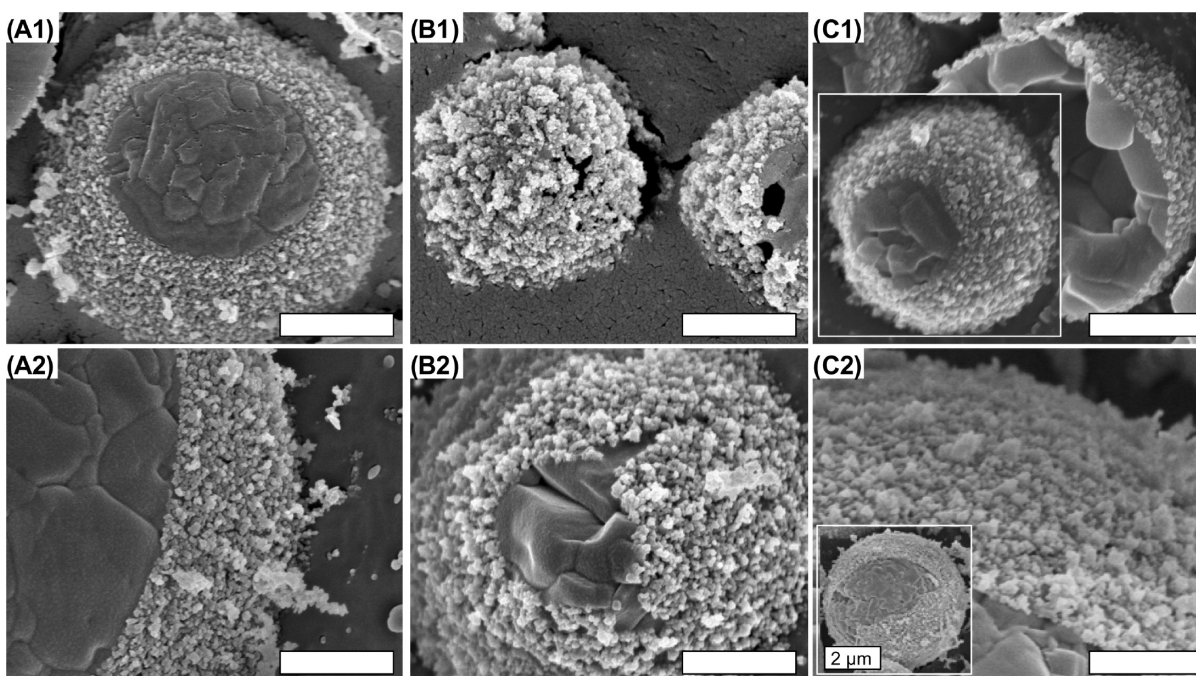


**Figure 6.** Cryo SEM images of dodecane droplets stabilized with alumina–PMAA particles (A1–C1)  $pH_C$  4 and (A2–C2)  $pH_C$  5. Corresponding pH values of emulsions are (A1) 4.8, (B1) 3.7, (C1) 2.4, (A2) 4.6, (B2) 4.3, and (C2) 3.0. Cross sectional views of the droplets are due to the sample preparation method. Length of unlabeled scale bars equals 500 nm.

increases the rate of particle deposition on the interface as well as the apparent nanoparticle number concentration; however, because we observe a decreasing droplet size with decreasing pH, the improved particle wettability seems to be a more significant factor influencing the average droplet size.

By comparing size distributions of different PE coating thicknesses ( $pH_C$  values) but the same emulsion pH values between pH 3.5 and 6, less broad droplet size distributions (SI) with a smaller average droplet size can be obtained with thicker PE coatings (smaller  $pH_C$  values). This can be explained by the increasing quantity of hydrophobic moieties with thicker PE coatings and the more efficient screening of the hydrophilic surface of the bare alumina particles.

The average droplet size reaches a minimum between pH 4.5 and 5.5 ( $0.15 < \alpha < 0.45$ ) for all  $pH_C$  values. For  $pH_C$  6, particles are flocculated, but for  $pH_C$  4 and 5, particles are not flocculated at this minimum. One can say that in the range of the minimum

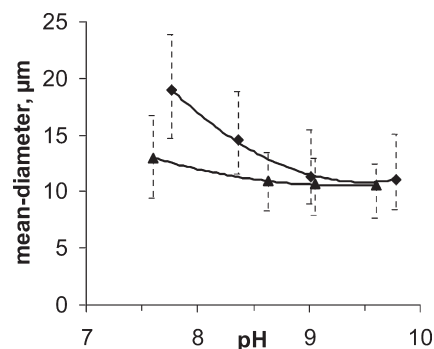


**Figure 7.** Average volumetric diameter of dodecane/water emulsion droplets stabilized by PAH-coated silica nanoparticles with different coating pH values  $pH_C$ :  $\blacklozenge$ ,  $pH_C$  8.5;  $\blacktriangle$ ,  $pH_C$  9.5. Lines are drawn to guide the eye. Dashed bars give upper and lower diameter at 50% height of the size distributions, not the error bars.

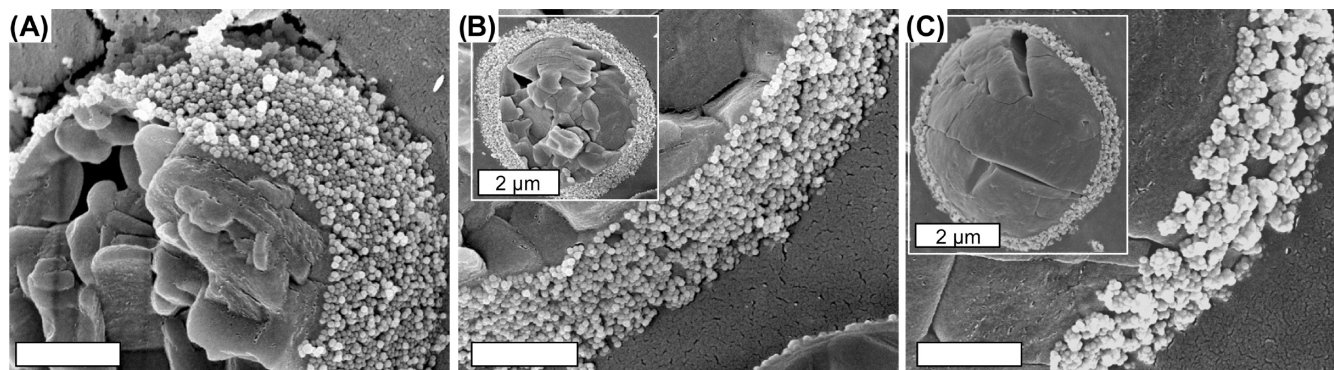


**Figure 8.** Cryo SEM images of dodecane droplets stabilized with silica–PAH particles of  $\text{pH}_C$  9.5. Corresponding pH values of emulsions are (A) 8.5, (B) 9.1, and (C) 9.8. Length of unlabeled scale bars equals 500 nm.

the particles provide the best properties to shift the competition between droplet stabilization and coalescence during emulsification toward stabilization. In the minimum for particles with the thickest PE coating ( $\text{pH}_C$  4,  $4.2 < \text{pH} < 5$ ), the smallest average droplet diameter can be obtained for the system alumina–PMAA and dodecane. Here the well-balanced wetting properties provide high stability against coalescence, and because of the low c.f.pH of 4.1, almost exclusively unflocculated individual droplets also exist. (See the SI.)

The average droplet size for all PE coating thicknesses increases again beyond the minimum ( $\text{pH} < 5$ ). Strong particle aggregation, reducing the apparent nanoparticle number concentration, occurs over the pH range with increasing average droplet size. For further discussion on the average droplet-size dependency on the pH, particularly for the region after the maximum, see the SI.

To investigate the effect of the oil phase polarity, we repeated our experiments with the more polar oil diethylphthalate. The benzene and ester functionalities give this molecule a more polar character than the saturated alkane chain of dodecane. We investigated only pH values at the minimum of the average droplet size and found the differences between the average droplet sizes for different  $\text{pH}_C$  values to be much smaller (Figure 5B). Here even the relatively thin PE layer of  $\text{pH}_C$  6 provides sufficient affinity to the diethylphthalate–water interface to create highly stable emulsions with small droplet sizes. On one hand, this can be attributed to an increase in  $\theta_{ow}$  due to the higher oil polarity; on the other hand, the interfacial tension between water and oil also might play a role, which implies a reduced rate of coalescence.

The visualization of the droplet shell morphologies of dodecane droplets done by cryo-SEM measurements is shown in Figure 6 for different  $\text{pH}_C$  and emulsion pH values.

As can be seen in Figure 6 for emulsions prepared above the c.f. pH with particles of  $\text{pH}_C$  4 and 5, the droplet shell consists of partially aggregated alumina–PMAA particles forming a relatively ordered shell coverage. Just below the c.f.pH, the droplet shell consists of highly aggregated particles, which create a relatively disordered shell with varying thickness. Further below the c.f. pH, particularly for samples with  $\text{pH}_C$  4, aggregation is reversed, and the degree of order of the droplet shell increases again.

The dense packing of particles at the oil/water interface can be suggested to be a reason for particle aggregation during emulsification. The close approach of particles here can lead to aggregation due to van der Waals forces. The mechanical effects of the ultrasonic irradiation can remove aggregated domains from the interface back to the bulk suspension.

The emulsification ability of silica–PAH particles was investigated, and the average droplet sizes of dodecane/water emulsions

in dependence of the emulsification pH value for two different  $\text{pH}_C$  values are shown in Figure 7.

Unlike the system alumina–PMAA, a higher  $\text{pH}_C$  value stands for a thicker PE layer for silica–PAH because  $\alpha$  of PAH decreases with increasing pH.

The ability of silica–PAH particles to stabilize emulsions begins at a pH value of  $\sim 7.2$  with a corresponding  $\alpha^{37}$  of PAH of  $\sim 0.8$ , which is comparable to the system alumina–PMAA. Also, for emulsions prepared with silica–PAH, the average droplet size decreases with decrease in  $\alpha$ .

Above pH 9 ( $\alpha < 0.45$ ), the average droplet size reaches a minimum. Less-pronounced but still established is the fact that for the same emulsion pH, particles with thicker PE coatings (higher  $\text{pH}_C$  values) are capable of creating smaller droplets. Again, the same argument can be used that thicker PE layers provide more hydrophobic moieties to screen the hydrophilic surface of the bare particles.

Although emulsions obtained with silica–PAH are highly stable, the bigger average droplet size compared with that for alumina–PMAA indicates a less-pronounced lipophilicity of silica–PAH, even with the thickest PAH layer. Obviously, the methyl group in the PMAA monomer unit enables better emulsification by alumina–PMAA particles. An improvement of the emulsification ability of PAH-coated particles could be achieved when the PE coating step took place at a higher  $\text{pH}_C$  value. For the highest  $\text{pH}_C$  value of 9.5, the corresponding  $\alpha$  equals 0.34, whereby for alumina–PMAA at  $\text{pH}_C$  4, the corresponding  $\alpha$  is 0.08. To obtain this low value of  $\alpha$  and thereby a higher layer thickness, the PAH coating step would have to be done at  $\text{pH}_C$  10.6, which is not possible because of the solubility of silica under such alkaline condition. The same limitation is given for the emulsification ability of silica–PAH particles above pH 10.

Remarkable is the lower ability of silica–PAH particles to stabilize diethylphthalate/water emulsions. Stable emulsions could be obtained, but a fraction of  $\sim 5$  vol % of the diethylphthalate was not emulsified. This observation is not yet clarified.

The droplet shell morphology is shown in Figure 8 for different emulsion pH values.

Silica–PAH particles arrange themselves in a monolayer, which partially consists of some aggregates below pH 9.2. Above this pH value, flocculation of particles takes place; consequently, the droplet shell consists almost entirely of particle aggregates.

(37) Petrov, A. I.; Antipov, A. A.; Sukhorukov, G. B. Base–acid equilibria in polyelectrolyte systems: from weak polyelectrolytes to interpolyelectrolyte complexes and multilayered polyelectrolyte shells. *Macromolecules* **2003**, *36*, 10079–10086.

## Conclusions

The isoelectric point and the pH range of colloidal stability of particles with adsorbed weak PEs depend on the PE conformation varied via the pH during the adsorption step. A strongly coiled PE results in (i) a greater shift of the isoelectric point toward a pH value corresponding to a lower degree of PE dissociation and (ii) a broader pH stability range.

Particles with adsorbed weak PEs (polycation or polyanion) can stabilize oil/water emulsions. We have demonstrated this fact for the weak polyacid PMAA on positively charged alumina and for the weak polybase PAH on negatively charged silica. The emulsification characteristics are determined by the surface wettability of the particles and thereby mainly governed by the adsorbed PE layer. By doing contact angle measurements, we found the wettability to depend on the degree of dissociation of the PE shell. The formation of stable Pickering emulsions is possible in a pH range where the degree of dissociation of the adsorbed weak PE lies below 80%. The thickness of the adsorbed PE layer influences the properties of the emulsions with nonpolar oils, enabling for the thicker layer the formation of smaller droplets. The dependency of the droplet size on the emulsion pH value and the PE coating thickness is explained with arguments based on the particle wetting properties, the particle aggregation state, and the oil phase polarity.

There is an optimal pH window (degree of dissociation between 15 and 45%) for the emulsions where the smallest droplets can be obtained. Here, depending on the PE layer thickness, colloidally stable particles and therefore also nonfloculated droplets can be obtained.

Particles with highly charged bare surfaces carrying a totally uncharged PE layer are also able to stabilize emulsions. In this case, emulsions stable to creaming can be obtained because of the formation of a particle–droplet network.

Particles that carry PEs with additional nonpolar functional groups (e.g., methyl group) have better emulsifying ability.

There are numerous potential combinations of particles (oxides, nitrides, carbides, latexes, etc.) and adsorbed weak PEs (PAH, PAA, PMAA, PEI, HA, etc.) that allow Pickering emulsification.

**Acknowledgment.** We gratefully thank Dr. Bernd-Reiner Paulke for inspiring discussions and for providing the equipment for droplet size determinations. Dr. Martin Hollamby is gratefully acknowledged for careful proofreading of the manuscript. The research was supported by the NanoFutur program of the German Ministry for Education and Research (BMBF), Volkswagen Foundation, and EU FP7 project “MUST”.

**Supporting Information Available:** PE desorption test, size characterization of PE-coated particles, further discussion about the pH-dependent droplet-size distribution, calculation of the required amount of PMAA for adsorption, zeta potential dependency of alumina–PMAA for  $\text{pH}_C$  5, contact angles for alumina and alumina–PMAA ( $\text{pH}_C$  6), discussion about broadness of droplet-size distributions, and micrographs of emulsions. This material is available free of charge via the Internet at <http://pubs.acs.org>.